High Voltage Capacitor Discharge Tool with Configurable Setpoints

Javier Lopez-Marrero, Kealan Frost, Will Serface, and Zeeshan Asif

Dept. of Electrical Engineering and Computer Science, University of Central Florida, Orlando, Florida, 32816-2450

***Abstract* — High voltage, utility grade capacitor banks can store large amounts of residual energy. The presence of this energy can be dangerous when performing testing or maintenance on such banks in a laboratory setting. This paper presents a custom lab tool that is designed to safely discharge 1200V DC, utility grade, metal film capacitor banks in under 30 seconds. Additionally, the tool features user configurable setpoints to alter the overall discharge profile along with safety functions to protect from unsafe operating conditions. Overall system, hardware, and software design will be discussed along with data supporting targeted performance metrics.**

***Index Terms* — Power capacitors, discharges (electric), voltage measurement, condition monitoring, electric safety, embedded systems, printed circuit boards, electrical equipment testing**

I. Introduction

NextEra Energy deploys PVS980 inverter systems for use in the power grid. These inverters also utilize capacitor banks in their normal operation. As a result, testing, verifying, and maintaining the function of these banks is critical. As energy storage elements, it is possible that residual energy remains within the capacitors both before and after testing. Seeing as a single bank could be charged up to 1200V DC, this poses a serious safety concern while also impacting testing. In response, NextEra Energy sponsored and tasked a team of senior design students to design a prototype piece of laboratory equipment that could safely discharge the capacitor banks in under 30 seconds. This team included: Javier Lopez-Marrero, Kealan Frost, Zeeshan Asif, and Will Serface.

To be further specific, the designed system should be able to discharge a 1200V DC, 1650uF capacitor in under 30 seconds. The system should also be able to display status alarms to the user for various points of the discharge cycle. The different stages of the discharge cycle will also be configurable by the user via specific voltage setpoints in order to make alterations to the overall discharge profile. For protection, temperature sensing will be incorporated to ensure safe operating temperatures. Lastly, despite the tool being designed and built out by the senior design team for high voltage specifications, for safety reasons the team of students will only test the system with a capacitor charged to 12V DC. More formal high voltage testing will be undertaken by NextEra Energy after the end of the senior design course sequence.

II. Overview of the System

A. Hardware Block Diagram

The hardware system can be divided into four main parts: the discharge plate, the control PCB, the I/O PCB, and the power system.

The discharge plate consists of a quarter inch, 2ft by 1ft aluminum plate which is used to mount high voltage components and to interface with the high voltage capacitor. This includes the main discharge resistors, which dissipate the energy of the capacitor as heat, and the contactors, which will help control the discharge cycle through the use of three separate resistive stages in parallel. Each stage has a different resistance associated with it, so controlling which parallel branches are active at specific points in time allows the user to manipulate the circuit's RC time constant and thus change the discharge profile.

The Control PCB interfaces with the discharge plate to monitor the capacitor voltage and activate the contactors at specific voltage setpoints. This is mainly achieved through an isolated voltage sensing circuit which employs an isolation amplifier and ADC to accurately read the high voltage input while protecting other low voltage electronics. The control PCB also features a resistance temperature detector (RTD) connection to monitor the temperature of the discharge plate during operation. Both pieces of information (voltage and temperature) are then processed by our microcontroller to make control decisions for the contactors and to display information to the user.

The main way to show information to the user is through a five-inch thin film transistor (TFT) liquid crystal display (LCD). This display will show the current voltage level, the elapsed time, the current system temperature, and the user defined setpoints. To better interface with the display and to better facilitate user input, an I/O PCB was designed with button inputs and LED outputs. These PCB connects directly with the control PCB and allows the use of the buttons to

configure the system setpoints while also allowing the LEDs to provide another way of communicating the system status during the discharge process.

Lastly, the entire system is powered off of a wall outlet connection. A prebuilt power supply is used to convert the 120V AC line voltage into 24V DC to power the control PCB. From there, two custom voltage regulator PCBs are used to regulate the voltage down to 3.3V and 5V for use in the low voltage electronics. These regulator PCBs plug directly into the control PCB to ease maintenance and troubleshooting.

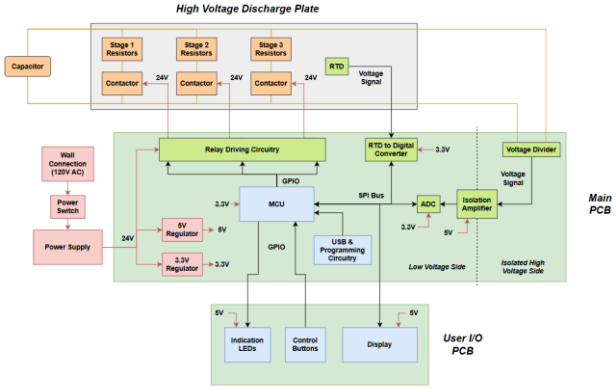

Figure 1 System Hardware Block Diagram

B. System Enclosure and Mechanical Design

With all the various subsystems and the presence of high voltage components, it became crucial to package all the components in a robust and safe manner. Since the discharge plate, along with the high voltage components mounted on it, occupied the most space, it naturally became the base of the system. From here, the enclosure was built upwards with six-inch aluminum standoffs, on top of which a quarter inch acrylic panel was mounted. This panel was customized with cutouts and mounting holes for holding the power supply and low voltage electronics. Side panels were also mounted onto the top acrylic in order to prevent any user from touching high voltage components. Machining for the acrylic and the mounting holes of the discharge plate was conducted by the UCF Machine Shop.

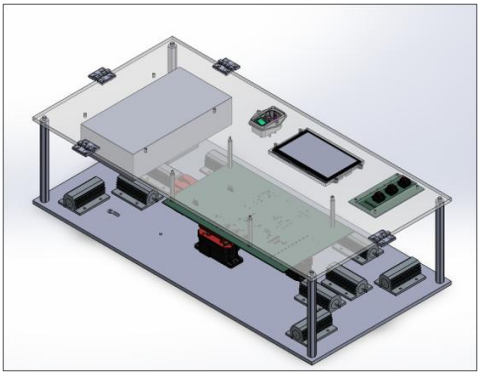

Figure 2 Current system enclosure CAD without side panels

III. Major Hardware Components

A. Power Resistors and Their Configuration

The discharge resistors selected for this tool were the HSC100, aluminum housed, wire wound from TE Connectivity, which are specifically designed for pulse and high voltage applications. Their free air power rating of 50W was an especially important factor when it came to their voltage handling capabilities (along with the resistance being considered). This is based on the following equation:

$$V = \sqrt{PR} \tag{1}$$

The resistor values used to achieve each stage resistance were: 2.5kΩ, 4.7kΩ, and 470Ω. These values at a 50W power rating give each resistor a maximum voltage rating of 353V, 484V, and 153V respectively. To stay within these ratings, multiple resistors were configured in either series or parallel to help divide the voltage. More specifically, the first stage resistor network includes four 2.5kΩ resistors in series (giving an equivalent stage 1 resistance of 10kΩ), the second stage includes a parallel combination of two 4.7kΩ resistors in series (giving an equivalent stage 2 resistance of 4.7kΩ), and the third stage includes four 470Ω resistors in series (giving an equivalent stage 3 resistance of 1.88kΩ).

B. Contactors

The contactors selected for tool were the P115 MINITACTOR from Sensata Technologies. This selection was made from a pure cost perspective, as it was one of the cheapest contactors on the market that could support switching for 1200V DC. Additionally, the form factor was small and convenient for mounting onto the discharge plate.

C. RTD and the RTD to Digital Converter

In discharging the system, we are converting electrical energy to thermal energy. To ensure that the power resistors and discharge plate do not get to unsafe temperatures, we implemented thermal sensing by way of RTD (Resistance Temperature Detector) probe and RTD to Digital Converter.

We selected the TT4-PT1000B platinum RTD probe and the MAX31865 RTD-to-digital converter. The TT4 probe was recommended by our sponsors and chosen mainly for its ring terminal, allowing for easier mounting by bolt directly to the aluminum discharge plate. The probe is rated for temperatures up to 125C, which covers our expected operating range and emergency cutoff values.

The MAX31865 is the excitation and conversion IC that pairs with our 1000 ohm probe[2]. It contains an internal ADC and bias current generator to provide the excitation for the probe and to generate the temperature value. The reference design is used to configure the supporting circuitry for the IC when in 2-wire and 1000 ohm probe mode, including connecting 2 of the output wires together and using a 4700 ohm reference resistor. The IC uses SPI to communicate with our MCU on a shared, parallel SPI bus.

D. Isolation Amplifier and ADC

The voltage sensing system must accurately measure the capacitor's voltage while maintaining isolation between the capacitor and the rest of the circuit. A resistive voltage divider is used on the high side that scales the capacitor's voltage down to ±1V, the input range of the AMC3330 precision isolation amplifier. The AMC3330 was selected for its integrated voltage reference, integrated high side power transfer, and high isolation rating of 4250 Vrms[3].

The output of the AMC3330 is a differential voltage ranging from -2V to +2V. Because of our target operating maximum input voltage rating of 1500V and how it scales through the AMC3330, we needed a linear, high-precision external ADC. The ADS1120 was chosen for its 16-bit resolution, internal reference, differential input measurement capability, and SPI communication protocol output. These together made the ADS1120 integrate very easily, not needing much external circuitry.

E. Microcontroller

The ESP32-WROOM-32D was chosen as our system's microcontroller. It has a dual-core processor that runs at 240 MHz, 520 kB of RAM, 4 MB of flash storage, and an internal 12-bit ADC. Our project is straightforward and minimal in terms of logic and computation. It reads SPI data from two sensors, prints to a screen over SPI, and uses GPIO pins for relay switching, button input, LED output, and peripheral data ready/select pins. The ESP32 provides enough general purpose I/O to perform all that is needed with headroom for further development or integration. The ESP32 is also highly recommended by Dr. Weeks and past senior design members for its familiarity, availability of replacement units, and prior success.

In designing around the ESP32, the reference designs show all the appropriate decoupling capacitors and connections needed to power the device. Also included in the reference designs was the programming and reset circuitry including an auto programmer and the CP2102N USB-to-UART converter bridge to streamline firmware flashing.

F. Display

When interacting with the tool, users can view information relevant to the device's state and real-time measurements of voltage and temperature on a graphical user interface built into the top panel of the system's enclosure. The display selected to perform this function is the NHD-5.0-800480FT-CTXL-T, which is a 5-inch, 800x480 LCD panel with a built-in FT812 graphics coprocessor. While the display does support touchscreen operations, users may wear PPE such as gloves that interfere with their ability to interact with the device using touch.

Using the shared SPI bus, the main ESP32 microprocessor sends commands to the display's coprocessor, which then renders a frame and outputs to the display panel, allowing the ESP32 to spend less time on UI and requires fewer GPIO pins compared to running the display directly.

On the display, the user sees the live voltage and temperature reading measured plus either a menu to configure the voltage setpoints of the discharge sequence, or a graph of voltage over time once they have confirmed the parameters. Additionally, if the program detects a potentially unsafe condition, a relevant message informs the user of the detected problem.

G. User Input Buttons and Output LEDs

To facilitate easy user interaction, Cherry MX Switch buttons were chosen as the main user input device. The final system contains three of these buttons for display navigation: an up button, a down button, and a select button.

For output to the user, LEDs are utilized in conjunction to the display to provide clear indication of when the various discharge stages activate and when the safe threshold voltage is reached. Different color LEDs are utilized to show progression in the discharge sequence. Stage 1 activation is indicated by the color red, Stage 2 and 3 are indicated by the color yellow, and the safe voltage being reached is indicated by the color green.

H. Power Supply and Regulators

The Power supply selected for use was the Nuwoniede Power Supply. This selection was made for a variety of purposes, dealing with functionality, spacing, and implementation within the system. The power supply needed to have an earth ground space in addition to the standard 120V AC voltage input and 24V DC output spaces. It was necessary to provide the discharge plate with an earth ground connection in case of fault conditions so that fault current has a low resistance path to flow without damaging other components.

For regulated voltages to be provided to the rest of the components, the LM 2576 switching regulator was selected as the final choice. This regulator, meant to provide both 3.3 volt and 5 volt regulation, requires a circuit with input and output capacitors. Voltage from the power supply would be provided as an input voltage to the regulator which would then buck the voltage down to a usable value for components such as the MCU, display and amplifiers.

IV. PCB Design

A. Control Board

The control/main board was designed in KiCad as a two-layer, 1 oz copper board. It is divided into two distinct regions: a high voltage section for the HV connectors, resistive divider, and isolation amplifier and a low voltage section for the ESP32 and all peripherals. The high voltage section does not feature a widespread internal ground plane, instead only having it where needed under the AMC3330. Under the isolation amplifier between each side of pins, a slot was milled to increase the creepage distance to properly accommodate our voltage rating. Creepage and clearance spacings were taken into account on all connections, resistors in the divider, and isolation amplifier on the high voltage side.

On the low voltage side, a continuous ground pour was used. Trace widths were sized according to the IPC-2221 standard as well as senior design guidelines according to their current loads[1]. Zero ohm resistors were used at possible disconnection points, and 47 ohm resistors were used on high speed lines to reduce ringing. Test point clips were included throughout the board on every main voltage and signal line to assist in testing/debugging. Components were spaced to give plenty of room for hand soldering and rework with the lab's available equipment.

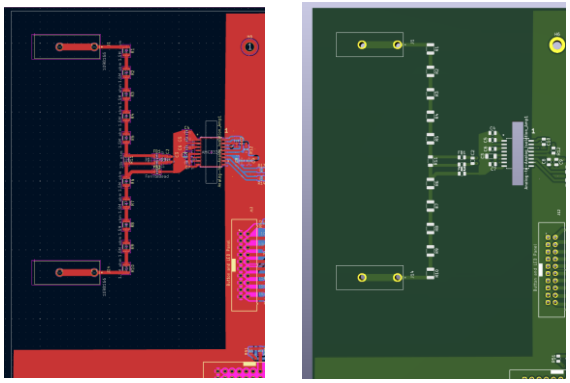

Figure 3 Layout and Model of High Voltage Isolated Section

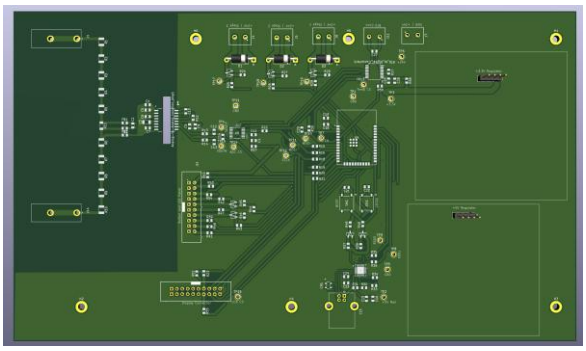

Figure 4: Main PCB Model

B. I/O Board

The I/O Board was realized on two-layer PCB. All of the connections were routed on the top layer, with a ground pour added over top. The bottom layer was used to mount the 20-pin through-hole header for connection to the main control PCB. All the extra space on the bottom layer was used to pour a uniform ground plane, which is stitched the top layers ground pour through all of the through-hole components (header and buttons). In assigning the pins to the 20-pin header, ground connections were added to spare pin counts and were placed in between signal lines to allow for greater EMI immunity.

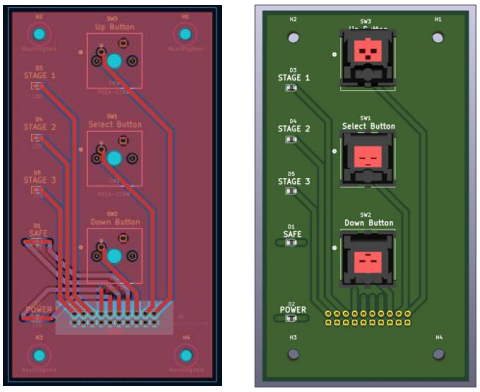

Figure 5 Layout and Model of IO Board

C. Regulators

The Regulator Boards were developed on two-layer PCBs. Two boards, one for 3.3 volts and one for 5 volts were designed respectively. The LM2576 header had 5 pins, outrouting to the input and output voltage as well as ground. The input capacitor and diode were placed as close as possible to the LM 2576 header for the sake of EMI management. Additionally, since more current was required of the 3.3 volt circuit, as it was providing voltage to more components such as the display, an extra input capacitor was placed in parallel with the first input capacitor. High frequency capacitors were also placed near the input and output capacitors to better manage efficiency overall. A 4-pin header is also placed to provide connections, in terms of the input and output voltages, to the main board.

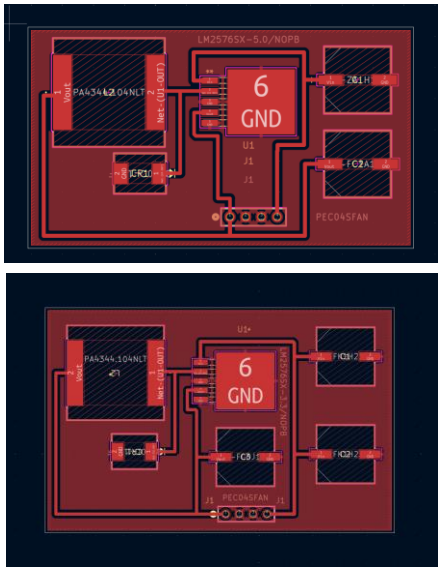

Figure 6: Layouts of Regulator Boards

D. Test Bank

For ease of testing, a two-layer capacitor bank PCB was also designed. The bank includes two screw terminals, one for charging the bank off a power supply and another for the output voltage. There is also a switch to disconnect the bank from the power supply once the charging is complete. Like the I/O Board, a ground pour was used on the top and bottom layer and stitched together through the through-hole components.

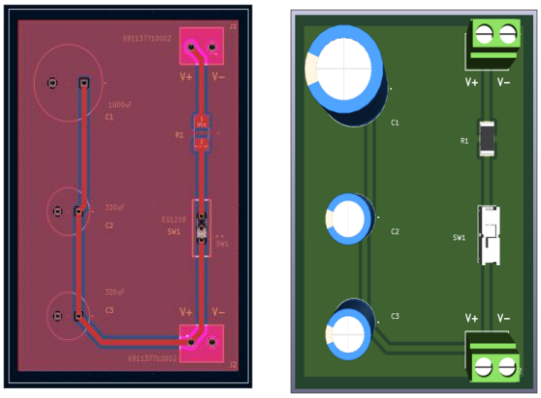

Figure 7: Layout and Model of the Test Bank Board

V. SOFTWARE DESIGN

When designing the software for the tool, the ESP32's Arduino integration was selected as the platform to implement the software. While it does reduce the maximum performance of the processor, the ESP32 model uses had more than sufficient performance overhead for the requirements of the program. Therefore, the programming language used for the system's software is C++ with augmentations provided by the Arduino and ESP32 platforms.

A. State Machine

Considering the use case of the tool, the state machine implemented by the program can be grouped into three major phases: first waiting on the user to configure the voltage setpoints (Configuration); then performing a sequence of actions informed by live data (Discharge); and finally notifying the user of the results (Completion).

Once the ESP32 has powered on, it enters the Configuration phase, where it presents the user with a menu that can be navigated using the three buttons, two for directional (up and down) navigation and one to select the highlighted option. This was implemented by creating two states for each adjustable option, one

where the user has highlighted the setpoint and the other allows the directional inputs to adjust the setpoint's value once selected. There are also two standalone states for when the selected menu option is to reset the customized values and to start the discharge sequence with the current values.

Figure 8: Configuration Phase Flowchart

During each of the three states in the Discharge phase, the program sets the corresponding relays of the current state to perform a safe discharge, saves the voltage and temperature measurements, and uses the data to generate a graph of the discharge curve. Once the measured voltage drops below the stage's set threshold, the program advances to the next state in the discharge sequence. Finally, once the measured voltage across the discharge network is less than 10V, the program enters the Completion phase, where it continues to display the graph of voltage over time recorded during the Discharge phase in addition to the latest voltage and temperature. If there were no issues, all relays will remain engaged until the user presses the select button to return to the Configuration menu.

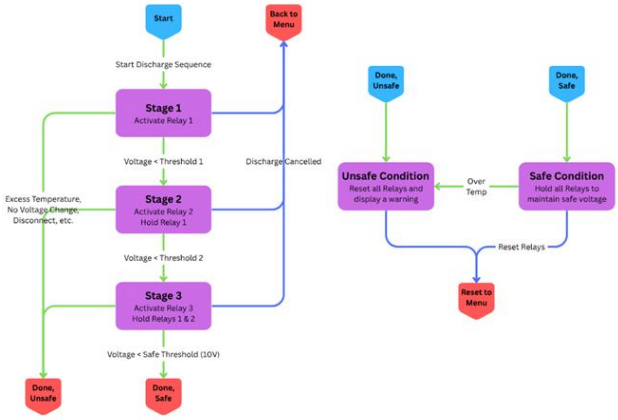

Figure 9: Discharge & Completion Flowcharts

B. *Classes & Data Structures*

To statically define all ten possible states of the program, the State enumeration is represented by one byte and is used to identify the current state of the program. This is augmented by the Threshold class, which represents the value of a voltage setpoint, along with the minimum and maximum values that it can be adjusted by the user.

Additionally, the program uses classes defined in libraries including Arduino platform's HardwareSerial and SPIClass interfaces for communication with peripherals such as USB programming and reading the voltage sensing ADC respectively. There are two libraries from third parties used in the program: Adafruit's MAX_31865 library, which supports RTD operations such as voltage to temperature conversion; and an open-source graphics library for controlling the display coprocessor and LCD.

VI. System Testing

A. *Regulator Performance*

The regulator efficiency, given the performance specifications of the design, was meant to be 80% or better. To test the accuracy of the regulators, an electronic load was connected to the PCB board and thus directly connected to the circuit, and the resulting voltage output was measured after a certain amperage of current was loaded. The current load ranged from 0 amps to 1.5 amps while the measured voltage was read directly off the display of the system and the overall

efficiency calculated to record 16 data points. Both regulators showed nearly 80% efficiency.

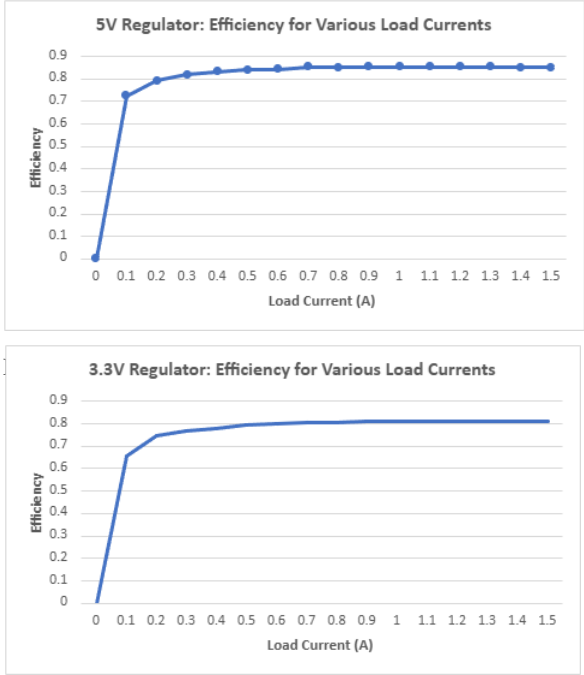

Figure 10: Efficiency versus load current for regulators

Another test was taken regarding the voltage regulation of the regulator. Starting off at 24V, the voltage input was progressively lowered in order to test the dropout voltage, where the voltage output would suddenly drop to 0. The input voltage was lowered from 24 V to 0V in 1 volt increments to record a total of 25 data points. For both designed regulators, dropout begins to occur around 5V. Considering the typical input for the designed regulators is 24V, the margin between the nominal input voltage and dropout is quite large.

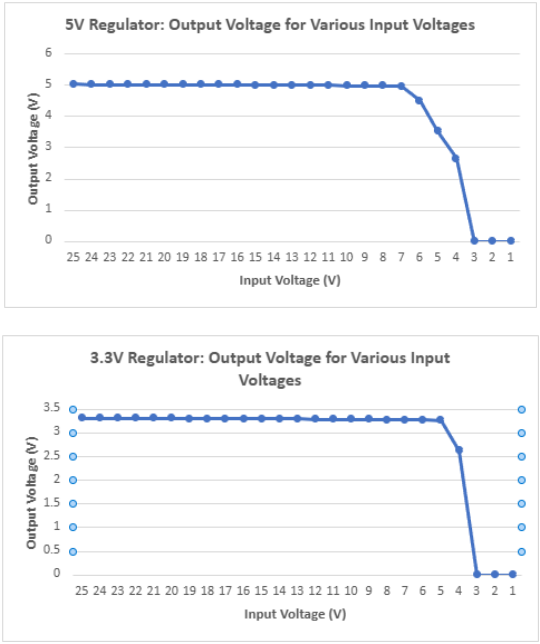

Figure 11: Voltage regulation for regulators

B. *Voltage Sensing Accuracy*

The error tolerance set for the voltage sensing system was to have less than a 5% inaccuracy. To test the accuracy of the system, a DC power supply was directly connected to the input of the system, as opposed to a capacitor bank. The measured voltage was read directly off the systems display and compared to the pre-set voltage of the power supply. The voltage was varied from 15V to 0V in 0.5V increments to record a total of 30 data points.

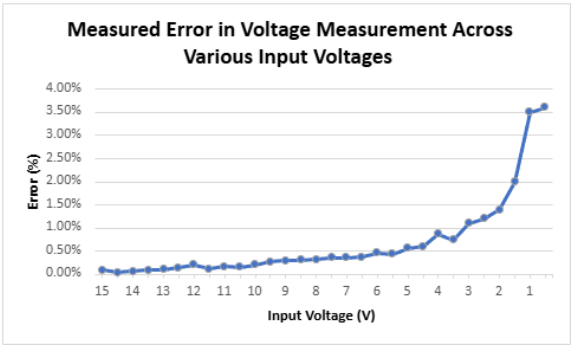

Figure 12: Voltage measurement error across range

Based on all the data, the system's voltage measurement is never more than 5% inaccurate compared to the actual input voltage. On average, the error is roughly 0.67% across all the data points. It is, however, worth noting that the error does increase significantly when approaching lower voltages. The highest error seen was at 0.5V which measured in at 0.518V. This translated to an error of 3.6%. This increase in error would likely not carry over when the device is scaled to higher voltages, however, since the set "safe" voltage would be 10V as opposed to 0.1V.

C. *Temperature Sensing Accuracy*

The error tolerance we set for the temperature sensing system was less than 10% inaccuracy. To test the accuracy, we attached the RTD probe and a thermocouple to a thermal mass. We then started to heat the thermal mass with a heat gun and measured the readings on both the RTD and thermocouple measurement device. Across all data points, a maximum inaccuracy of 8% was found which is within our specification. It should also be noted that the probes may heat up differently and could not be placed in the same location, which may account for some of our observed inaccuracies.

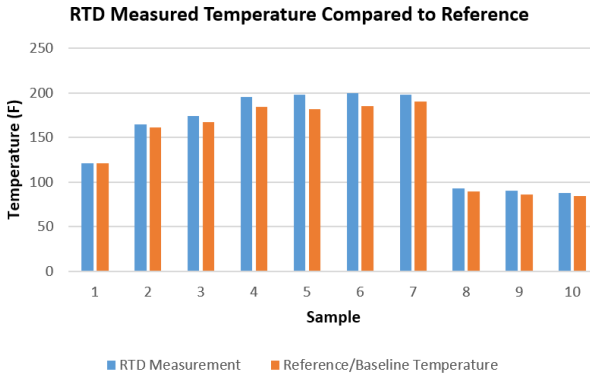

Figure 13: RTD Measurement versus reference

D. Discharge Time

To measure the discharge time and its accuracy, the system was run under various operating conditions. Input voltage was varied along with stage voltage setpoints. Overall discharge time was then compared with an LTSPICE simulation of the system. The setup for this simulation can be seen below, along with an example of what the simulation results typically look like.

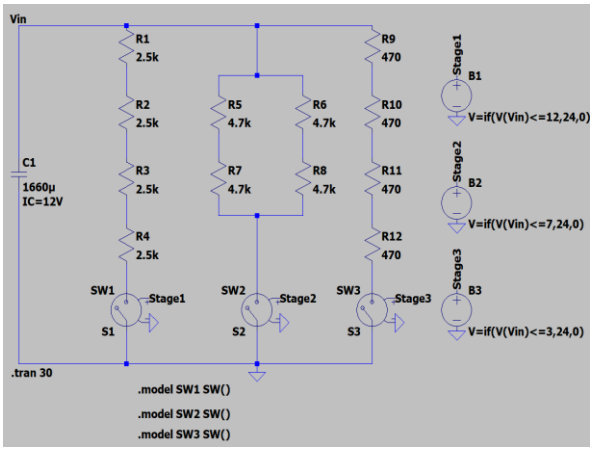

Figure 14: LTSPICE circuit of discharge system

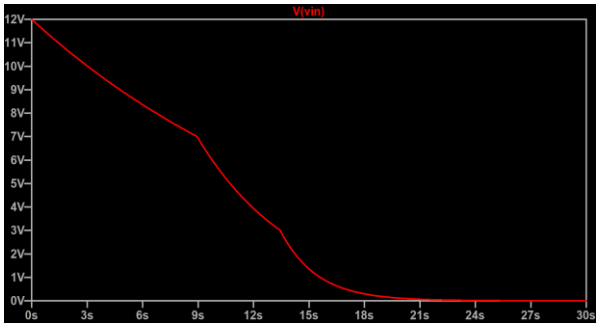

Figure 15: Example LTSPICE Simulation Result

To compare the measured discharge time with the simulated discharge time, the voltage setpoints for the system were fixed. With the fixed setpoints, five trials were conducted at a set starting input voltage (ie: five trials done for Vin = 12V, five trials done for Vin = 9V, etc.). The discharge times for each of the five trials were then averaged together and the average time was compared to the simulated discharge time for the specific starting voltage used. This process was then repeated for different voltage setpoints. Overall, the measured discharge time was always under the target of 30 seconds. Real discharge times were usually around two seconds longer than theoretical times, which is expected considering that the simulation does not consider components tolerances, parasitic resistance in wire and solder joints, and processing delays in the MCU.

VII. Conclusion

The system components discussed, along with the shown PCB design and software design, constitute an effective system for removing residual voltage from capacitor banks. Data from testing highlights that the performance of the system is within expected tolerances. Future high voltage verification will be conducted by NextEra Energy.

Acknowledgments

The authors wish to acknowledge Dr. Chung-Yong Chan, Dr. Arthur Weeks, Dr. Gabrial Vazquez-Ramos, Gerardo Acosta, Nicholas Wayne, and Sharon Campbell. Additionally, the authors wish to acknowledge NextEra Energy's Power Generation Division (PGD) for this sponsorship of this project.

References

[1] IPC, "IPC-2221A: Generic Standard on Printed Board Design," Association Connecting Electronics Industries, Bannockburn, IL, 2003.

[2] Analog Devices, "MAX31865 RTD-to-Digital Converter Datasheet," [Online]. Available: https://www.analog.com/media/en/technical-documentation/data-sheets/max31865.pdf

[3] Texas Instruments, "AMC3330 Precision Isolation Amplifier Datasheet," [Online]. Available: https://www.ti.com/lit/ds/symlink/amc3330.pdf